2011 American Control Conference
on O'Farrell Street, San Francisco, CA, USA
June 29 - July 01, 2011

Simulation Study of a Novel Self-Powered Active Suspension System for Automobiles

K. Singal and R. Rajamani

Abstract - **It has been shown in literature that a semi-active automotive suspension system can provide significant benefits compared to a passive suspension but cannot quite match the performance of a fully active suspension. However the advantage of a semi active suspension is that it consumes negligible energy and utilizes a variable damper whose damping coefficient is changed in real time, while a fully active suspension consumes significant power for its operation. This paper explores a new zero energy active suspension system that combines the advantages of the active and semi-active systems. Unlike a semi-active system in which the energy is always dissipated using a variable damper, the proposed system harvests and recycles energy to achieve active operation. It is found that the system performs as well as the active system with energy to spare for higher frequencies, while at low frequencies (below 0.8 Hz) there is inadequate energy for fully active operation.**

I. INTRODUCTION

For decades, researchers have studied the performance enhancement of automotive suspensions using active and semi-active systems. It has been long established that active and semi-active suspensions can provide substantial performance improvements over optimized passive suspensions [1]. Though the performance of an active system, in general, is superior to that of a semi-active system, it consumes significantly more power than semi-active systems [2] and hence there is a tradeoff. It is however interesting to note that significant energy is typically dissipated in the shock absorbers of a passive suspension system. For example, the dissipated energy of four dampers of a passenger car traversing a poor roadway at 13.4 m/s reached approximately 200W [3, 4].

A couple of systems have been proposed to utilize this dissipated energy [5-10]. Nakano et. al. [7] proposed to control active vibrations using energy absorption with two linear DC motors. One was placed in the primary suspension, acted as an energy regenerative damper, while the other placed in the secondary suspension was used for active vibration control. The author then implemented this system on a truck suspension system [6]. Though a novel idea, the realization of this system is complex due to the presence of a mechanical energy regenerative damper in the primary suspension. The same authors also implemented the system using a single DC motor placed in the secondary suspension [8]. For the control scheme they used a variable resister and a condenser to store the absorbed energy with three stage control logic.

Kawamoto et. al. [9] suggested an alternative electromagnetic damper (EMD) consisting of a DC motor and a ball screw mechanism. The EMD has high controllability and can be used for both active suspension and energy regeneration. The authors proposed to use a variable control voltage to control the current in the circuit.

In all these papers, the authors performed energy analysis, presented dynamic models for the elctro-mechanical system and presented simulation results. However, they did not implement a fully self-powered vibration control system.

This paper proposes to implement a zero-energy active suspension system using a single electrical motor/generator which tries to achieve the performance of an externally powered fully active suspension. The performance of this system is then compared to the fully active system and a passive system at different frequencies.

II. SYSTEM MODEL

The system was modeled as a two degree of freedom quarter car system with a single electromagnetic motor/ generator [9], acting both as an actuator and energy harvesting mechanism. A two degree of freedom quarter car suspension model is shown in Figure 1 and its parameters are summarized in Table 1.

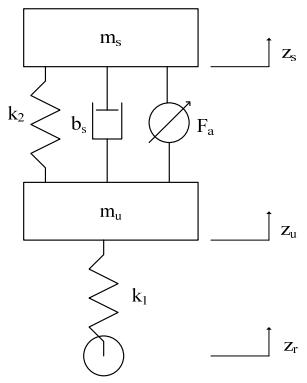

Figure 1: Quarter car suspension model

The authors are with the University of Minnesota, Minneapolis, MN 55455, (Email: ksingal@me.umn.edu, rajamani@me.umn.edu)

The equations of motion for this system driven by a force, F_a, are given by equations (1) and (2).

$$m_s\ddot{z}_s = -b_s(\dot{z}_s - \dot{z}_u) - k_2(z_s - z_u) + F_a \quad (1)$$

$$m_u\ddot{z}_u = b_s(\dot{z}_s - \dot{z}_u) + k_2(z_s - z_u) + k_1(z_r - z_u) - F_a \quad (2)$$

Symbol	Description
m_s	Sprung mass
m_u	Unsprung mass
k_1	Tire stiffness
k_2	Suspension stiffness
b_s	Damping coefficient
F_a	Control Force
z_s	Displacement of sprung mass
z_u	Displacement of unsprung mass
z_r	Road input
ω	Angular velocity of motor shaft
l	Lead of ball screw
T_l	Load torque required

Table 1 : Parameters of suspension

The actuation and energy harvesting is performed using the motor-generator. Figure 2 shows a diagram of the electromagnetic system. The motor is assumed to be fixed to the sprung mass of the car and the nut is mounted to the unsprung mass. The relative motion between the two is converted into a rotary motion of the screw, which acts as a shaft for the motor.

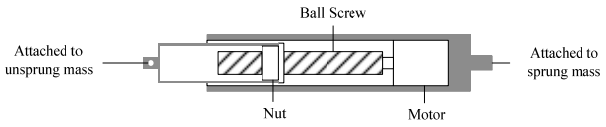

Figure 2: Schematic of actuator and energy harvesting system

The relation between relative motion of the sprung and unsprung masses of the car to the angular velocity of the screw is given by equation (3)

$$\omega = \frac{2\pi(\dot{z}_s - \dot{z}_u)}{l} = k_l(\dot{z}_s - \dot{z}_u) \quad (3)$$

and that between the torque exerted by the motor and the force exerted on the sprung and unsprung masses of the car is given in (4)

$$F_a = \frac{2\pi T_l}{l} = k_l T_l \quad (4)$$

The DC motor circuit used in the system can be modeled as shown in Figure 3 and its parameters are listed in Table 2.

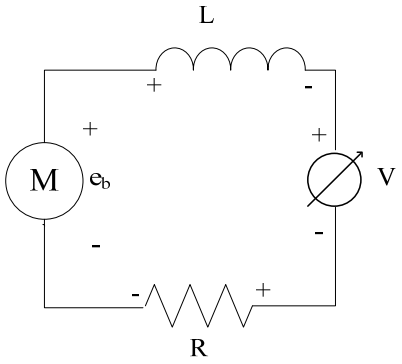

Figure 3: Circuit Diagram of Motor

Symbol	Description
R	Resistance
L	Inductance
M	Motor
V	Variable control voltage
I	Current
e_b	Back emf
k_e	Back emf constant
k_t	Torque constant
T_e	Electromagnetic torque

Table 2 : Parameters of suspension

The variable voltage source can be implemented using a power electronic converter to up-convert/down-convert the voltage of a battery. The equations of this circuit are given by equations (5) - (7)

$$e_b = k_e\omega \quad (5)$$

$$L\dot{I} = -RI - V + e_b \quad (6)$$

Ignoring the inertia and damping of the DC motor,

$$T_l = T_e = k_t I \quad (7)$$

III. CONTROLLER DESIGN

The desired active force, F_a^{des}, is controlled using the control law for "sky-hook" damping, which is given by equation (8).

$$F_a^{des} = -4000\dot{z}_s \quad (8)$$

As this F_a^{des} is to be provided by the DC motor, we can convert it to an equivalent desired torque, T_{des} and an equivalent desired motor current, I_{des}. These are given by equations (9) and (10).

$$T_{des} = \frac{F_a^{des}}{k_l} \tag{9}$$

$$I_{des} = \frac{T_{des}}{k_b} = \frac{F_a^{des}}{k_b k_l} \tag{10}$$

A control law can then be formulated to control the voltage of the variable voltage source, V, so that the current, I, tracks the desired current, I_{des}. A proportional-integral (PI) controller is used for this purpose. The control law is given by equation (11).

$$V_{des} = -\left(K_p + \frac{K_i}{s}\right)\left(I_{des} - I\right) \tag{11}$$

The actual voltage may or may not be equal to the desired voltage of equation (11), depending on the sign of IV_{des} and the available amount of harvested energy in the battery. The algorithm to determine the actual voltage is described in Figure 4. In Figure 4, the desired force, F_{des}, is first calculated from using the "sky-hook" law. This force is then translated into a desired control voltage, V_{des}, using equations (9) – (11). The instantaneous power requirement, IP, is calculated. Depending upon the sign of IP, the battery can be seen as supplying energy to the system (discharging) or withdrawing energy from the system (charging) . At the start of the simulation it is assumed that the energy in the battery is zero. The simulation was implemented so that it forces V to zero whenever the IP is negative (i.e. to control the system we have to supply energy from battery) and the energy available in the battery is below a low threshold. In all the other cases V is set to V_{des}. After applying the control voltage, V, the actual current, I, and energy in the battery, E, are estimated.

IV. RESULTS

A road input of magnitude 0.1 m and frequencies ranging from 0.1 Hz to 30 Hz were used to evaluate the performance of the controller. The performance of the system was compared with the active and passive systems.

Figure 5.a compares the acceleration of the zero-energy system to that of active and passive systems for a road disturbance of 1 Hz, it can be seen that the performance of the system is comparable to that of the active system. But a quick glance at figure 5.b shows that the system has not reached the steady state yet. Figure 5.c and 5.d shows the acceleration and energy respectively from 25 seconds to 30 seconds, here it is clearly visible that the steady state has been reached, but the system is not able to fully give a performance equal to that of the active system. After reaching steady state, we observed that the battery was charging for 43.93% of the time and that we could supply the required control voltage for 86.02% of the time. This tells us that for 13.98% of the time the system was running in energy deficit, which explains the reason for the lower performance as compared to the active system.

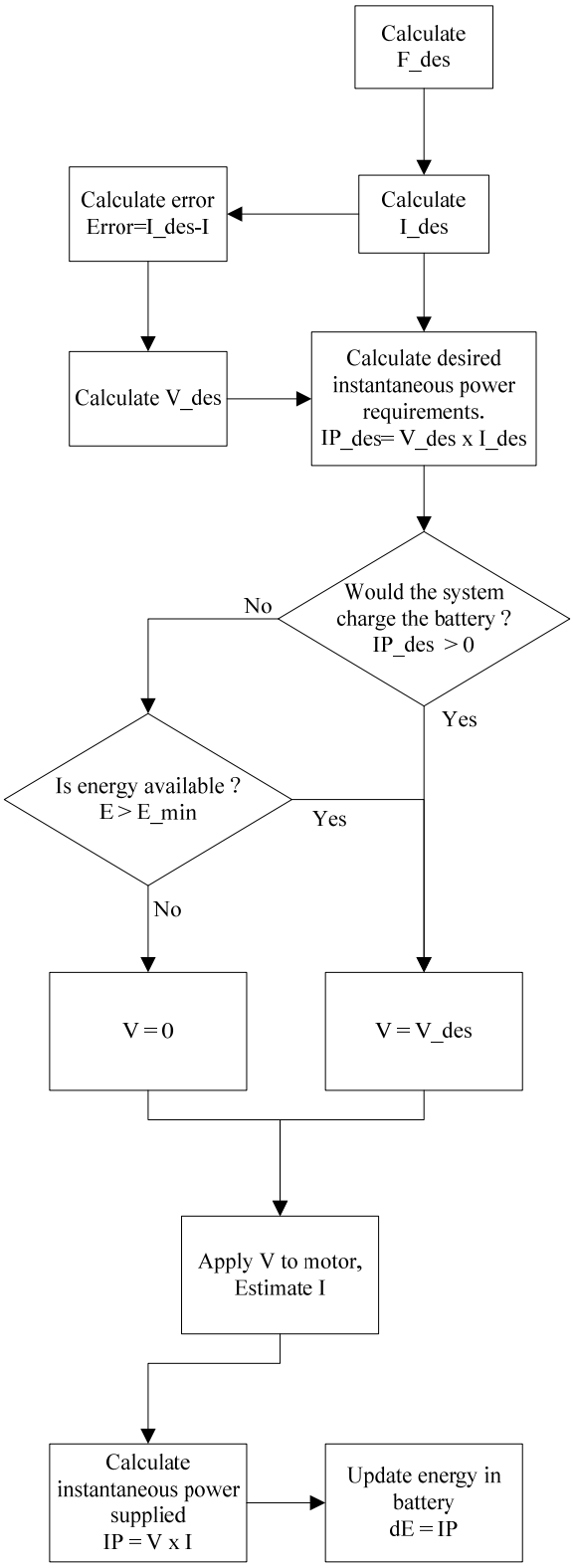

Figure 4 : Algorithm for determining the control voltage

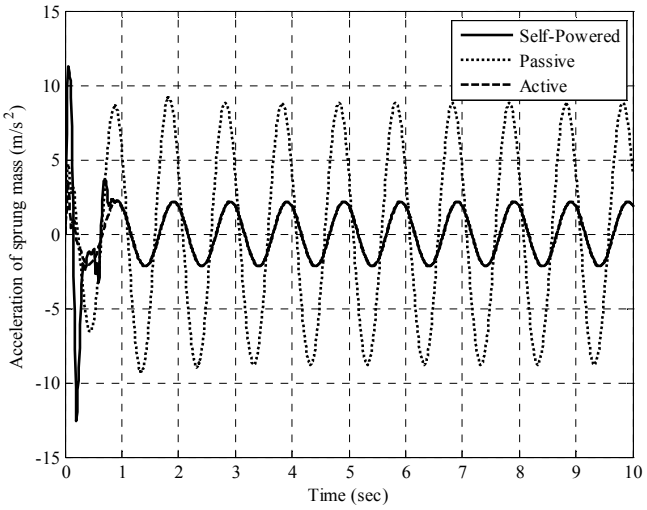

Figure 5.a: Acceleration of sprung mass for active, passive and zero-energy active system for a road disturbance of 1 Hz.

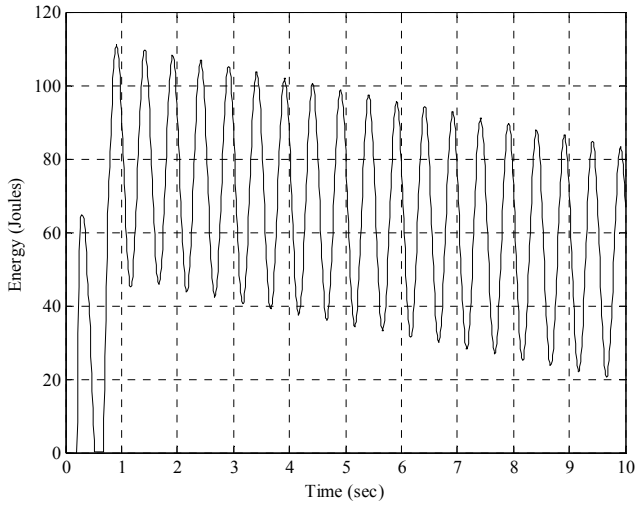

Figure 5.b: Energy in the storage battery for a road disturbance of 1Hz

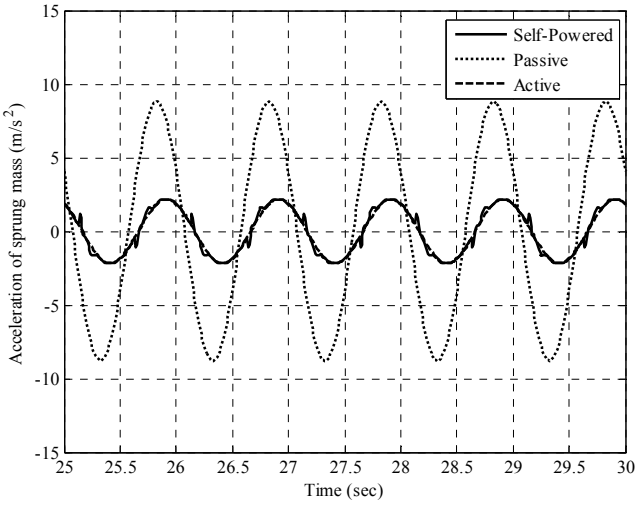

Figure 5.c: Acceleration of sprung mass for active, passive and zero-energy active system for a road disturbance of 1 Hz from 25 to 30 seconds.

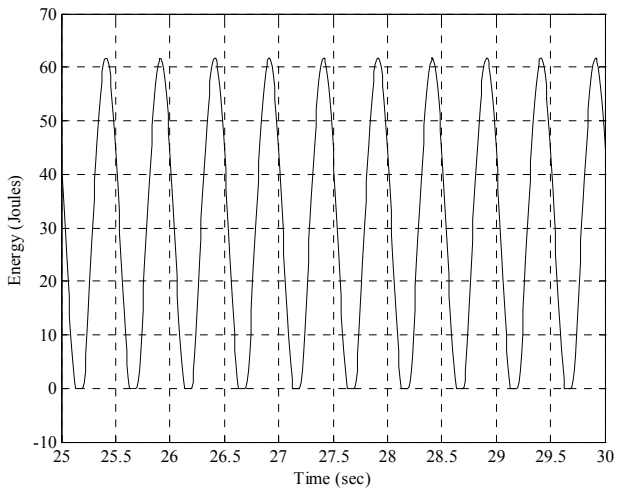

Figure 5.d: Energy in the storage battery for a road disturbance of 1Hz from 25 to 30 seconds.

Figures 6.a and 6.b show the acceleration of sprung mass and energy stored in the storage battery respectively for a road disturbance of 2 Hz. We can see that the system is able to perform upto the levels of an active system. For 2 Hz, for 30 seconds of simulation, we observed that after reaching steady state the battery charged for 51.91% of the time and we could supply the required control voltage for 100% of the time. On the other hand, plots of the acceleration of sprung mass and energy in the storage battery for a road input of 0.75 Hz, figures 7.a and 7.b respectively, show that there is some deficiency of energy and hence there is a minor degradation in performance. Here the battery charging time and the time for which we were able to apply control voltage was found to be 42.43% and 84.53% respectively. As we further decreased the frequency to 0.5 Hz, these percentages went down to 45.52% and 82.36% respectively. The acceleration of sprung mass and energy in the storage battery for this frequency are shown in figures 8.a and 8.b respectively. As can be seen the performance of the system has degraded quite a bit and is now at times worse than the passive performance.

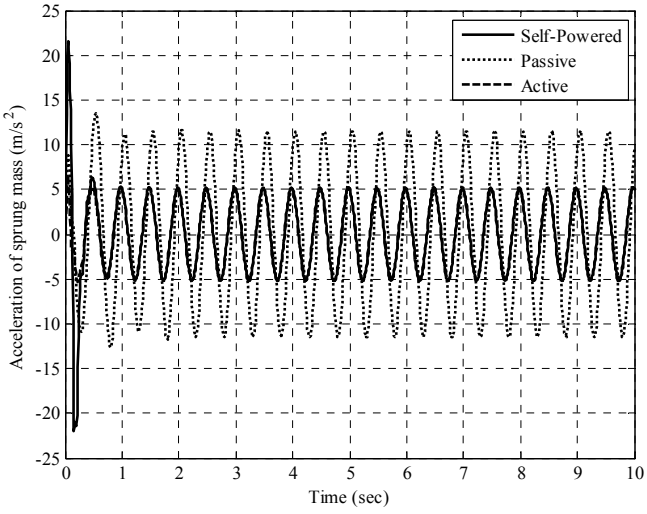

Figure 6.a: Acceleration of sprung mass for active, passive and zero-energy active system for a road disturbance of 2 Hz.

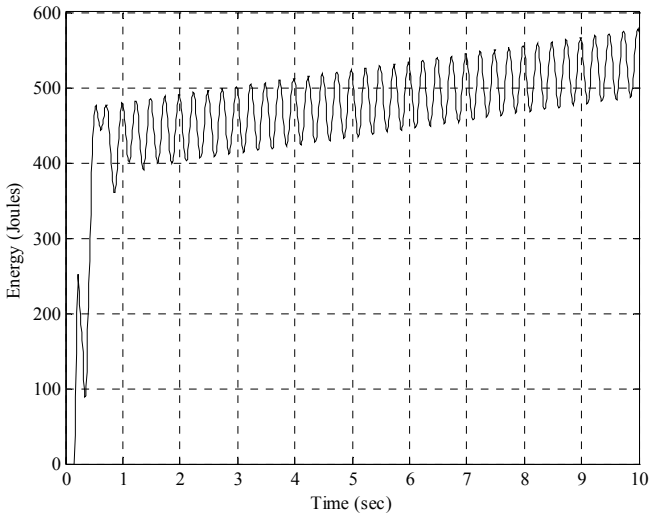

Figure 6.b: Energy in the storage battery for a road disturbance of 2Hz

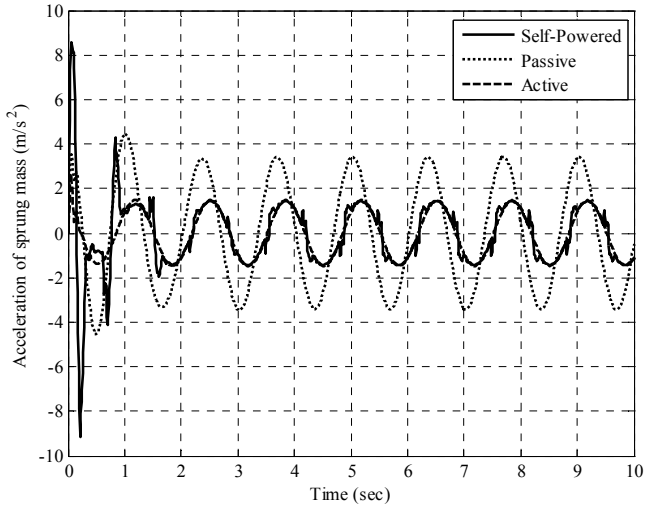

Figure 7.a: Acceleration of sprung mass for active, passive and zero-energy active system for a road disturbance of 0.75 Hz.

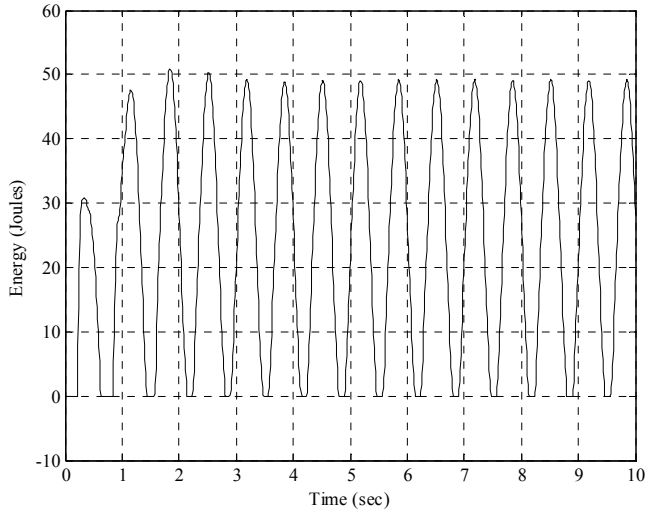

Figure 7.b: Energy in the storage battery for a road disturbance of 0.75Hz

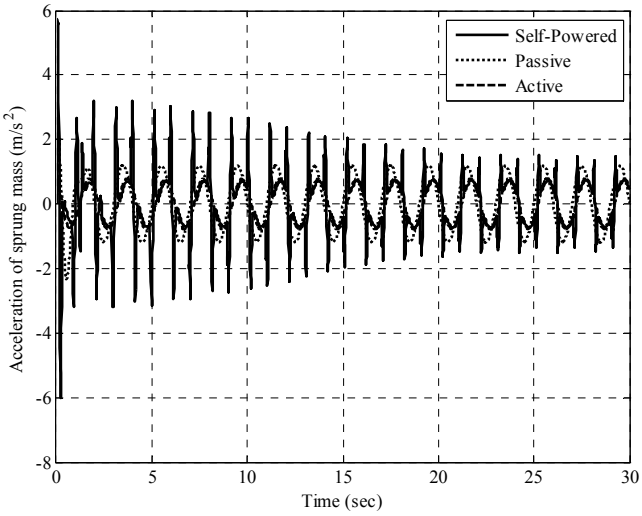

Figure 8.a: Acceleration of sprung mass for active, passive and zero-energy active system for a road disturbance of 0.5 Hz.

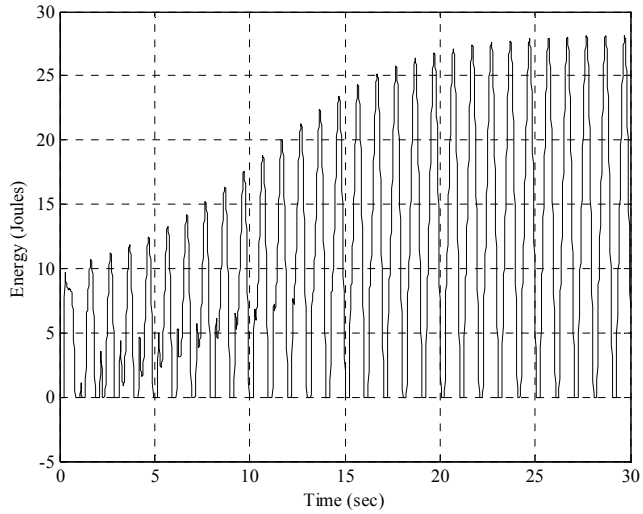

Figure 8.b: Energy in the storage battery for a road disturbance of 0.5Hz

Figure 9 shows the transfer function magnitude of sprung mass acceleration as a function of frequency. Due to the presence of higher frequency content at low excitation frequencies, the peak value of acceleration in the steady state, irrespective of frequency content, was considered while plotting this graph. As can be observed, the zero-energy system performance equals the performance of the active system for frequencies above 1.2 Hz. Between 0.8 Hz and 1.2 Hz, the performance is almost equal to that of the fully active suspension system. Between 0.5 Hz and 0.8 Hz, the performance is in between passive and active system while below 0.5 Hz the system performs worse than the passive system. Figure 10 shows the fraction of time when the battery is charging and when energy is available to implement the active system. It confirms our observation that at frequencies higher than 1.2 Hz, a fully active system can be implemented as the energy is available for utilization at all times. At frequencies below 0.5Hz, the system has inadequate energy.

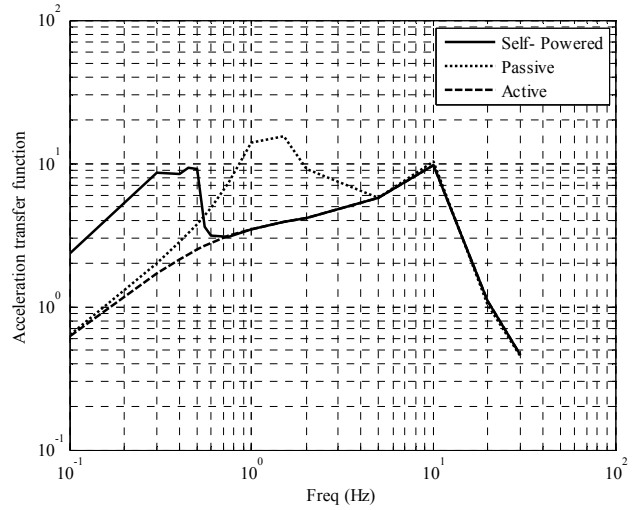

Figure 9: Acceleration transfer function as a function of frequency of road disturbance

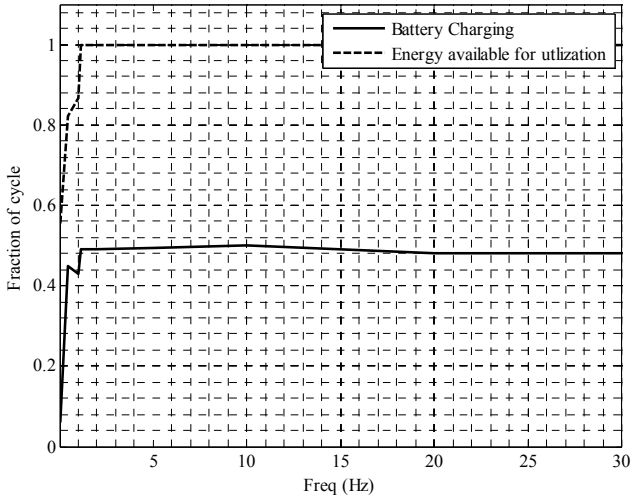

Figure 10: Fraction of times the battery is charged and fraction of time energy is available to implement active system.

V. CONCLUSIONS

This paper explored the idea of a zero-energy active suspension using a single electromagnetic motor-generator. The system was simulated for a range of frequencies and its performance was compared to the fully active and passive systems. The system could almost deliver the performance of a fully active system for road disturbances of frequency 0.8 Hz or higher. At frequencies below 0.5 Hz, the performance of the system was worse than that of the passive system. The performance below 0.5 Hz can be improved to be equivalent to that of the passive system by using high-pass filters to implement active control only at higher frequencies.

REFERENCES

[1] K. Yi and B. Song, "A New Adaptive Sky-Hook Control of Vehicle Semi-Active suspensions," *Proceedings of the Institution of Mechanical Engineers -- Part D -- Journal of Automobile Engineering,* vol. 213, pp. 293-303, 05/18, 1999.

[2] R. Rajamani, *Vehicle Dynamics and Control.* Springer, 2006.

[3] M. G. Fodor and R. C. Redfield, "The variable linear transmission for regenerative damping in vehicle suspension control," in *American Control Conference, 1992,* 1992, pp. 26-30.

[4] L. Segal and Xiao-Pei, "Vehicular resistance to motion as influenced by road roughness and highway alignment," *Australian Road Research,* vol. 12, pp. 211-222, 1982.

[5] Y. Suda, S. Nakadai and K. Nakano, "Hybrid Suspension System with Skyhook Control and Energy Regeneration (Development of Self-Powered Active Suspension)," *Veh. Syst. Dyn.,* vol. 29, pp. 619-634, 01/02, 1998.

[6] K. Nakano, Y. Suda, S. Nakadai, H. Tsunashima and T. Washizu, "Self-powered active control applied to a truck cab suspension," *JSAE Rev.,* vol. 20, pp. 511-516, 10, 1999.

[7] K. Nakano, Y. Suda and S. Nakadai, "Self-Powered Active Vibration Control Using Regenerated Vibration Energy," *Journal of Robotics and Mechatronics,* vol. 11, pp. 310-314, 1999.

[8] K. Nakano, Y. Suda and S. Nakadai, "Self-powered active vibration control using a single electric actuator," *J. Sound Vibrat.,* vol. 260, pp. 213-235, 2/13, 2003.

[9] Y. Kawamoto, Y. Suda, H. Inoue and T. Kondo, "Modeling of Electromagnetic Damper for Automobile Suspension," *Journal of System Design and Dynamics,* vol. 1, pp. 524-535, 2007.

[10] M. Montazeri-Gh and M. Soleymani, "Investigation of the Energy Regeneration of Active Suspension System in Hybrid Electric Vehicles," *Industrial Electronics, IEEE Transactions on,* vol. 57, pp. 918-925, 2010.